

## **Seismic Vulnerability Assessment of Asymmetrical Reinforced Concrete Buildings in Australia**

E. Lumantarna<sup>1,3</sup>, A. Mehdipanah<sup>1,3</sup>, N. Lam<sup>1,3</sup>, H.H. Tsang<sup>2,3</sup>, J. Wilson<sup>2,3</sup>, E. Gad<sup>2,3</sup> and H. Goldsworthy<sup>1,3</sup>

<sup>1</sup> Department of Infrastructure Engineering, The University of Melbourne, Parkville, Victoria, Australia

<sup>2</sup> Faculty of Science, Engineering and Technology, Swinburne University of Technology, Melbourne, Victoria, Australia

<sup>3</sup> Bushfire and Natural Hazards Cooperative Research Centre (BNHCRC)

### **ABSTRACT:**

Many reinforced concrete buildings in Australia are laterally supported by reinforced concrete cores/shear walls that are eccentrically located in the buildings. The structural elements at the edges of the asymmetrical buildings can be subjected to a significant displacement demand, making this type of buildings highly vulnerable in an earthquake. Seismic assessment methods for asymmetrical buildings commonly involve three-dimensional dynamic analyses that can be computationally expensive. This paper presents a simplified analysis method for multi-storey buildings featuring plan asymmetry. The method has been used to assess the seismic vulnerability of asymmetrical reinforced concrete buildings in Australia.

**Keywords:** asymmetrical buildings, simplified analysis method, fragility curves, reinforced concrete

## 1 INTRODUCTION

Reinforced concrete buildings make up the majority of Australian's building stocks. The buildings are commonly designed with little to no considerations of ductile detailing and often feature vertical and/or plan irregularities. Seismic design guidelines and assessment procedures (e.g., Eurocode 8 (EN 1998-1, 2004), AS 1170.4-2007 Commentary (Standards Australia, 2009), FEMA 450-1 (Building Seismic Safety Council, 2003), FEMA 356 (ASCE, 2000)) require dynamic analyses to be performed on such structures. However, modelling of irregular buildings is complex and requires expert judgment. There are also currently no consistent guidelines on the selection of ground motion inputs for the analyses.

The authors have recently developed a simple and accurate method (referred to as the Generalised Lateral Force Method) for the analysis of multi-storey buildings (Mehdipanah *et al.*, 2016). The method has been shown to be able to provide estimates of the displacement demand on multi-storey buildings less than 30 m in height. The robustness of the method has been demonstrated on multi-storey buildings featuring vertical irregularities that are caused by discontinuities in the gravitational load carrying elements.

In this paper, the method has been extended to account for the effects of torsion caused by plan asymmetry. Dynamic analyses can be computationally expensive especially as far as three-dimensional dynamic analysis is concerned and hence the developed method will provide significant time savings in the seismic assessment of this type of buildings. The dynamic torsional behaviour has been the subject of research since the 1980s (e.g., Dempsey and Tso, 1982; Chandler and Hutchinson, 1988; Rutenberg and Pekau, 1987; Chopra and Goel, 1991; Tso and Zhu, 1992; Chandler and Duan, 1997). However, many of the findings of these studies are contradictory as they are largely dependent on the building models, parameters and assumptions adopted in the studies.

The method introduced in this paper is aimed at approximating results of dynamic analyses required by current codes of practice (e.g., AS1170.4-2007 (Standards Australia, 2007); Eurocode 8 (EN 1998-1, 2004)) assuming linear elastic behaviour. The displacement demands on the buildings can be estimated by applying the behaviour factor, or structural modification factor, in accordance with the codes. The developed method is introduced in Sections 2 and 3. Section 2 presents expressions that can be used to provide estimates of displacement at the edges of torsionally unbalanced (TU) buildings developed based on a single-storey building model. The expressions presented in Section 2 requires multi-storey buildings to be idealised into a single-storey building model. A method to obtain the idealised single-storey building model is presented in Section 3. The developed method has been verified by comparison with dynamic analysis results of two case study reinforced concrete buildings in Section 4. The method has been used to construct fragility curves for the two case study buildings in Section 5.

## 2 EDGE DISPLACEMENT OF TORSIONALLY UNBALANCED (TU) BUILDINGS

Estimates of the maximum displacement demand at the edges of TU buildings have been derived based on a single-storey building model with uni-axial asymmetry (Figure 1). The single-storey building model has been shown to be able to represent the torsional behaviour of multi-storey TU buildings (Anagnostopoulos *et al.*, 2015; Lam *et al.*, 1997).

The torsional response behaviour of a TU building is governed by a few parameters: i)  $e$  is the eccentricity; ii)  $K_x$  is the translational stiffness of the TU building; iii)  $K_\theta$  is the torsional stiffness of the TU building; iv)  $m$  is the mass of the TU building; v)  $J$  is the torsional mass

of inertia of the TU building ( $= mr^2$ ), where  $r$  is the mass radius of gyration. Parameter “ $b$ ” ( $= \sqrt{K_\theta/K_x}$ ) is used to represent the torsional stiffness properties of the TU building.

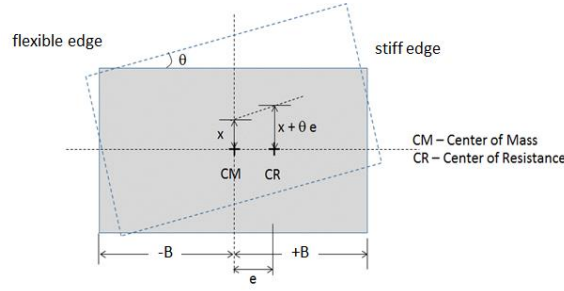


Figure 1 Uni-axial asymmetry single-storey building model

The maximum displacement demand at the edges of the TU building can be obtained by using dynamic modal analyses if linear elastic behaviour is assumed. The dynamic equilibrium for a uni-axial asymmetry single-storey building is provided by Equation (1):

$$\begin{bmatrix} 1 & 0 \\ 0 & 1 \end{bmatrix} \begin{Bmatrix} \ddot{x}_r \\ \ddot{\theta} \end{Bmatrix} + \omega_x^2 \begin{bmatrix} 1 & e_r \\ e_r & b_r^2 + e_r^2 \end{bmatrix} \begin{Bmatrix} x_r \\ \theta \end{Bmatrix} = \begin{Bmatrix} 0 \\ 0 \end{Bmatrix} \quad (1a)$$

$$\omega_x^2 \begin{bmatrix} 1 & e_r \\ e_r & b_r^2 + e_r^2 \end{bmatrix} \begin{Bmatrix} x_r \\ \theta \end{Bmatrix} - \Omega_j^2 \begin{bmatrix} 1 & 0 \\ 0 & 1 \end{bmatrix} \begin{Bmatrix} x_r \\ \theta \end{Bmatrix} = \begin{Bmatrix} 0 \\ 0 \end{Bmatrix} \quad (1b)$$

where,  $\ddot{x}_r$  and  $x_r$  are the translational acceleration and displacement, respectively, normalised with respect to the mass radius of gyration  $r$ ,  $\ddot{\theta}$  and  $\theta$  are the rotational acceleration and displacement respectively,  $\omega_x$  is the translational natural angular velocity of the uncoupled mode of vibration and  $\Omega_j$  is the natural angular velocity of the coupled modes of vibration.

Letting  $\lambda_j^2 = \frac{\Omega_j^2}{\omega_x^2}$ , the eigenvalue solution for Equation (1b) is given by:

$$\lambda_j^2 = \frac{1+(b_r^2+e_r^2)}{2} \pm \sqrt{\left[\frac{1-(b_r^2+e_r^2)}{2}\right]^2 + e_r^2} \quad (2)$$

The dynamic equation equilibrium (Eq. (1b)) has two eigenvalues solution.  $\lambda_1$  defines the first coupled natural angular velocity and is smaller than 1.0,  $\lambda_2$  defines the second coupled natural angular velocity and is larger than 1.0.

The eigenvector solution for Equation (1b) is given by:

$$\begin{Bmatrix} x_r \\ \theta \end{Bmatrix} = \begin{Bmatrix} 1 \\ \left(\frac{\lambda_j^2 - 1}{e_r}\right) \end{Bmatrix} \quad (3)$$

where,  $x_r = x/r$  and  $e_r = e/r$ .

Based on the eigenvalue and eigenvector solutions provided by Equations (2) and (3) and using the *square-root-of-the-sum-of-the-square* (SRSS) combination rule, the maximum displacement at the center of mass (CM) and center of rigidity (CR) positions and at the edges of the building (Figure 1) are provided by Equation (4). The SRSS combination rule has been shown to be able to provide reasonably accurate estimates of the maximum displacement demand of TU buildings (Lumantarna *et al.*, 2013).

$$x_{CM}(\max) = \sqrt{\sum_{j=1}^2 \frac{1}{1+\theta_j^2} \times RSD(T_j, \xi)} \quad (4a)$$

$$x_{CR}(\max) = \sqrt{\sum_{j=1}^2 \lambda_j^2 \frac{1}{1+\theta_j^2} \times RSD(T_j, \xi)} \quad (4b)$$

$$x_{\pm B}(\max) = \sqrt{\sum_{j=1}^2 \left(1 + \theta_j(\pm B_r)\right) \times \frac{1}{1+\theta_j^2} \times RSD(T_j, \xi)} \quad (4c)$$

where,  $x_{CM}$  is the maximum displacement at the CM of the building,  $x_{CR}$  is the maximum displacement at the CR of the building,  $x_{+B}$  is the maximum displacement at the stiff edge of the building (Fig. 2a) and  $x_{-B}$  is the maximum displacement at the flexible edge of the building (Fig. 2b).  $RSD(T_j, \xi)$  is the response spectral displacement value at the coupled modal period  $T_j$  of the building.

The maximum displacement of the TU building can be presented in the form of displacement ratio ( $\Delta/\Delta_o$ ).  $\Delta$  is the maximum displacement of the TU building at the edges and  $\Delta_o$  is the maximum displacement of the equivalent torsionally balanced (TB) building, the TB building which possesses translational stiffness equal to the translational stiffness of the TU building. The displacement can be represented by the response spectral displacement  $RSD(T, \xi)$  at the uncoupled modal period ( $T$ ) of the TU building. The displacement ratio is defined for the acceleration, velocity and displacement controlled conditions (presented schematically in Figure 2) by Equations (5):

$$\frac{\Delta}{\Delta_o} = \frac{x_{\pm B}(\max)}{RSD(T, \xi)} = \sqrt{\sum_{j=1}^2 \left[ \frac{1+\theta_j(\pm B_r)}{1+\theta_j^2} \times \frac{1}{\lambda_j^2} \right]^2} \quad (5a)$$

for the acceleration-controlled conditions,

$$\frac{\Delta}{\Delta_o} = \frac{x_{\pm B}(\max)}{RSD(T, \xi)} = \sqrt{\sum_{j=1}^2 \left[ \frac{1+\theta_j(\pm B_r)}{1+\theta_j^2} \times \frac{1}{\lambda_j} \right]^2} \quad (5b)$$

for the velocity-controlled conditions, and

$$\frac{\Delta}{\Delta_o} = \frac{x_{\pm B}(\max)}{RSD(T, \xi)} = \sqrt{\sum_{j=1}^2 \left[ \frac{1+\theta_j(\pm B_r)}{1+\theta_j^2} \right]^2} \quad (5c)$$

for the displacement-controlled conditions.

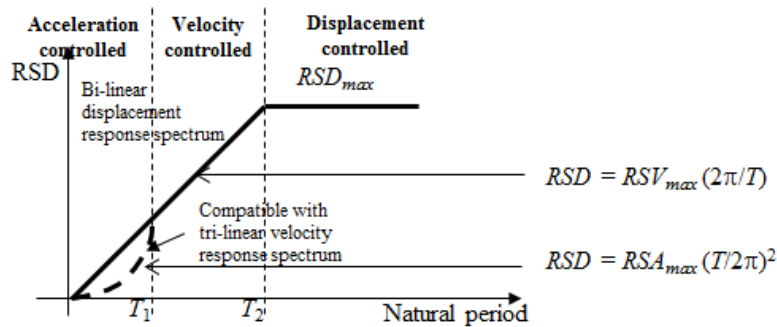


Figure 2 Displacement response spectrum featuring acceleration-, velocity- and displacement-controlled regions

### 3 IDEALISATION OF A 3-D TU BUILDING INTO A SINGLE STOREY BUILDING MODEL

The torsional behaviour of TU buildings can be represented by single-storey building models with similar torsional properties (represented by eccentricity ( $e$ ) and torsional stiffness

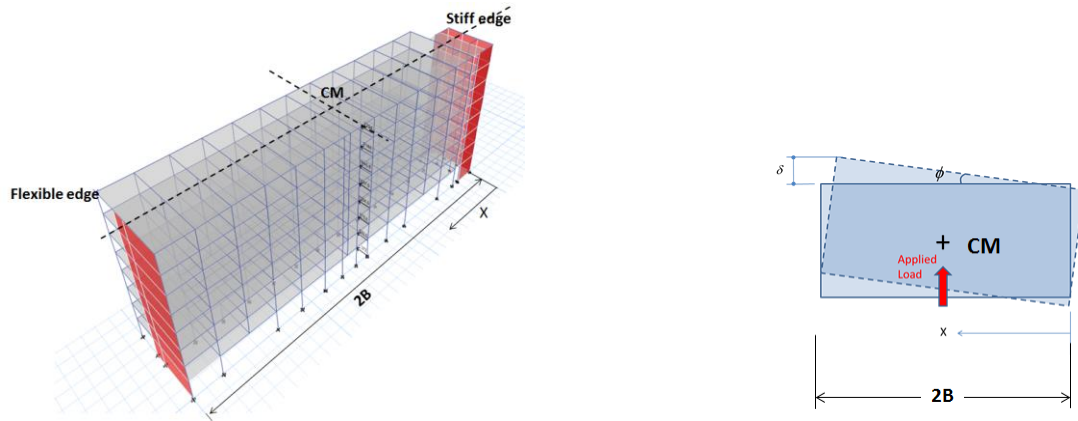
parameter ( $b$ )). Multi-storey buildings often feature discontinuities in their lateral and/or gravitational load carrying elements and consequently there can be a lot of variation in the mass, storey eccentricity and torsional stiffness values of the individual floors. A method to determine the values of  $e$  and  $b$  for the multi-storey building is presented in this section.

First, lateral load is applied at the center of mass (CM) of each floor as schematically shown in Figure 3a. The magnitude of the lateral load can be determined in accordance with seismic codes (e.g., AS1170.4-2007 (Standards Australia, 2007); Eurocode 8 (CEN, 2004)). The effective displacement of the multi-storey building model can be determined using Equation (6).

$$\delta_{eff} = \frac{\sum m_i \delta_i^2}{\sum m_i \delta_i} \quad (6)$$

where,  $m_i$  and  $\delta_i$  are the mass and displacement of floor  $i$ , respectively.

The maximum displacement ( $\delta$ ) and the rotation of the building ( $\phi$ ) as schematically shown in Figure 3b can be obtained based on the effective displacement at the edges of the building.

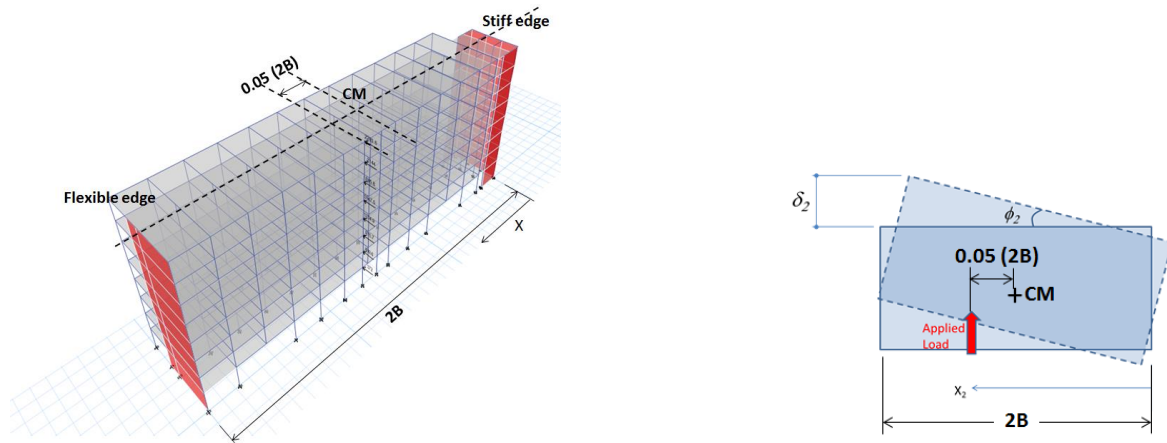


(a) three-dimensional view of the TU building model

(b) plan view of the TU building model

Figure 3 Applying lateral load at the CM of the TU building

Second, the lateral load is applied at an arbitrary location which is further away from the CM of the building (the load is shown to be applied at 0.05 of the building width ( $2B$ ) from the CM in Figure 4a). The maximum displacement ( $\delta_2$ ) and the rotation of the building ( $\phi_2$ ) (shown in Figure 4b) caused by the imposed lateral load can be obtained based on the effective displacement at the edges of the building.



(a) three-dimensional view of the TU building model

(b) plan view of the TU building model

Figure 4 Applying lateral load at an arbitrary point further away from the CM of the TU building

The CR of a building is a location on the building at which the lateral load applied will only result in translational displacement of the building ( $\phi = 0$ ). Based on the values of  $\phi$  and  $\phi_2$  the value of eccentricity  $e$  can be found by extrapolation as schematically shown in Figure 5. Similarly, based on the values of  $\delta$ ,  $\delta_2$  and  $e$  the value of the translational displacement ( $\Delta_o$ ) can be found by extrapolation (shown schematically in Figure 6).

The torsional stiffness parameter  $b_r$  (normalised with respect to the radius gyration of the building ( $r$ )) can be obtained from the relationship between the displacement edge ratio and the torsional parameters when a static load is applied at the CM of the building:

$$\frac{\Delta}{\Delta_o} = 1 + \frac{e_r}{b_r^2} B_r \quad (7a)$$

where,  $\Delta$  is the maximum displacement of the TU building subject to a static load applied at the CM ( $\Delta$  is equal to  $\delta$  shown in Figure 3b),  $\Delta_o$  is the translational displacement,  $e_r$  and  $b_r$  are the eccentricity and torsional stiffness parameter, respectively, normalised with respect to the radius of gyration of the building ( $r$ ).  $B_r$  is half of the width of the building (Figure 3a) normalised with respect to the radius of gyration of the building.

The torsional stiffness parameter  $b_r$  can be found by re-arranging Equation (7a):

$$b_r = \sqrt{\frac{e_r B_r}{\left(\frac{\Delta}{\Delta_o} - 1\right)}} \quad (7b)$$

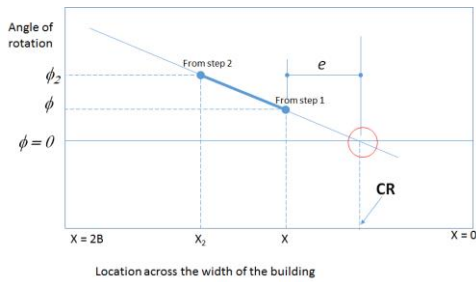


Figure 5 Finding the CR of the building

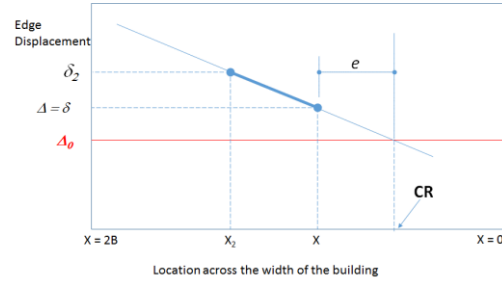
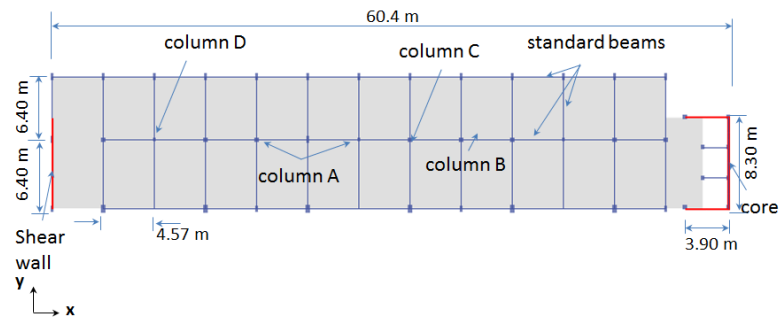


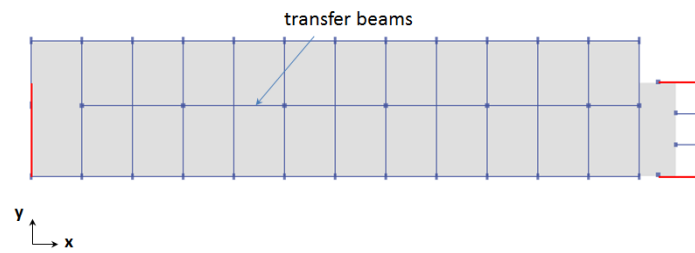
Figure 6 Finding the translational displacement ( $\Delta_o$ )

#### 4 COMPARISON WITH THE DYNAMIC ANALYSES OF CASE STUDY BUILDINGS

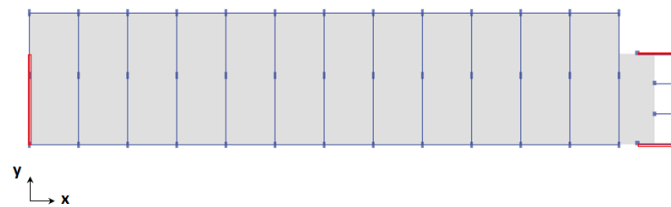
Three-dimensional dynamic analyses have been performed using program ETABS (Computer & Structures Inc. 2013) on a number of multi-storey building models to verify predictions based on the proposed method presented in Sections 2 and 3. Results of dynamic analyses on two buildings are presented in this section. The buildings are laterally supported by moment resisting frames and reinforced concrete shear walls. Some of the columns in the moment resisting frames of the buildings were discontinuous, resulting in vertical irregularities in the buildings. Figures 7 and 8 present typical plan views of the buildings. The three-dimensional views of the building models are presented in Figures 9 and 10. The height of the buildings was 28 m and 21.2 m, for buildings 1 and 2, respectively. The mass radius of gyration of the buildings was 18 m and 16 m, for buildings 1 and 2, respectively. The geometric and material properties of the elements of the buildings are summarised in Table 1. The mass and  $e_r$  values of the individual floors are listed in Table 2.



(a) ground floor

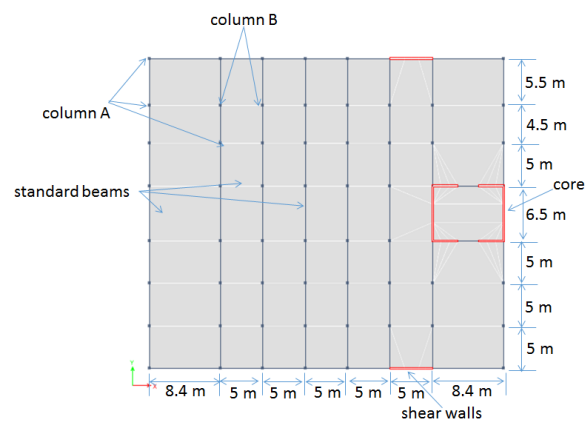


(b) floor 1 to 4



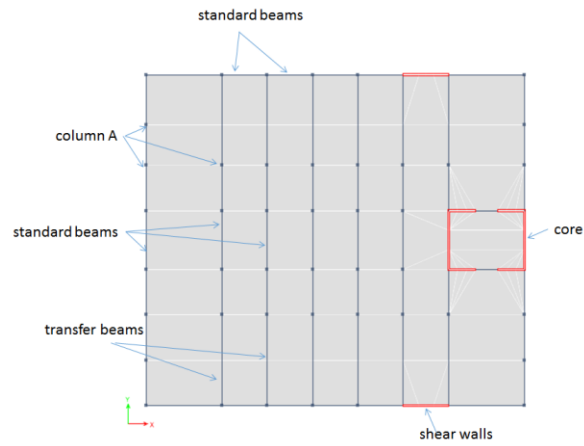
(c) floor 5 to roof

Figure 7 Plan view of Building 1



(a) typical floor

Figure 8 Plan views of Building 2



(b) floor 2  
Figure 8 cont'd

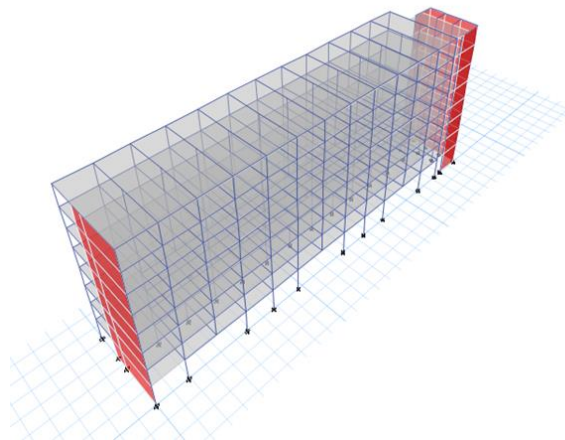


Figure 9 3-D view of Building 1

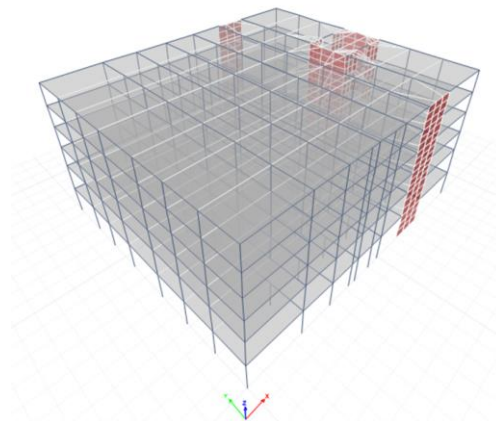


Figure 10 3-D view of Building 2

Table 1 Dimensions of principal structural elements and material properties (mm)

(a) Building 1

Element	Slab	Walls		Beams		Columns			
Type		Core	Shear	Standard	Transfer	A	B	C	D
Material	RC	RC	RC	RC	RC	RC	RC	RC	RC
Width (mm)	-	200	200	280	280	375	280	400	300
Depth (mm)	250	-	-	620	1000	810	610	400	300
Length (mm)	-			-	-				



(b) Building 2

Element	Slab	Walls		Beams		Columns	
Type		Core	Shear	Standard	Transfer	A	B
Material	RC	RC	RC	RC	RC	RC	RC
Width (mm)	-	200	200	280	300	350	300
Depth (mm)	250	-	-	450	1600	350	300
Length (mm)	-			-	-		

RC – reinforced concrete with modulus of elasticity of 24.5 GPa and density of 2500 kg/m<sup>3</sup>

Table 2 Storey mass, eccentricity and torsional stiffness of the building

(a) Building 1

Level	Storey mass (t)	Eccentricity	
		$e_r$	
		x-direction	y-direction
1	755	-0.07	0.14
2	738	-0.02	0.31
3	738	0.02	0.44
4	751	0.06	0.53
5	719	0.08	0.60
6	719	0.10	0.64
7	719	0.11	0.67
Roof	684	0.12	0.70

(b) Building 2

Level	Storey mass (t)	Eccentricity	
		$e_r$	
		x-direction	y-direction
1	1244	0	0.96
2	1228	0	0.95
3	1204	0	0.92
4	1198	0	0.91
5	1198	0	0.89
roof	1152	0	0.90

The dynamic analyses were conducted based on the design response spectrum in accordance with AS1170.4-2007 (Standards Australia, 2007) for site class C. The  $k_p Z$  value of 0.08g was adopted in the analyses. Results of the analyses are presented in the form of maximum deflection at the edges of the buildings in Figure 11. The maximum deflection values at the edges of the TU buildings were compared with the translational deflection of the equivalent TB buildings. It is shown that the variation in the storey  $e_r$  values do not have significant effects on the displacement shapes of the buildings. Despite the variation in the  $e_r$  values, the displacement shape of the TU buildings were shown to be similar to that of a TB building.

The method introduced in Sections 2 and 3 were used to provide estimates of the displacement response of the TU buildings. Lateral load in accordance with AS1170.4-2007 (Standards Australia, 2007) was applied at the CM and a point further away from the CM to determine the  $e_r$  values of the TU buildings. The buildings were assumed to be constructed on a class C site in Melbourne ( $k_p Z = 0.08$ ). The  $e_r$  values of the idealised single-storey building models in the direction of the earthquake ground motion were found to be 0.67 and 0.88, for buildings 1 and 2, respectively. The eccentricity of the buildings in the direction perpendicular to the earthquake ground motion was small and ignored in this study. Based on the  $e_r$  values for the building models, Equation 7(b) was used to determine the  $b_r$  values. As the fundamental periods of both buildings are in the velocity-controlled range of the response spectrum, Equations (2), (3) and 5(b) were used to calculate the displacement ratio for the

stiff and flexible edges of the buildings. The eccentricity  $e_r$ , torsional stiffness parameters  $b_r$  and the displacement ratio ( $\Delta/\Delta_o$ ) for both buildings are summarised in Table 3.

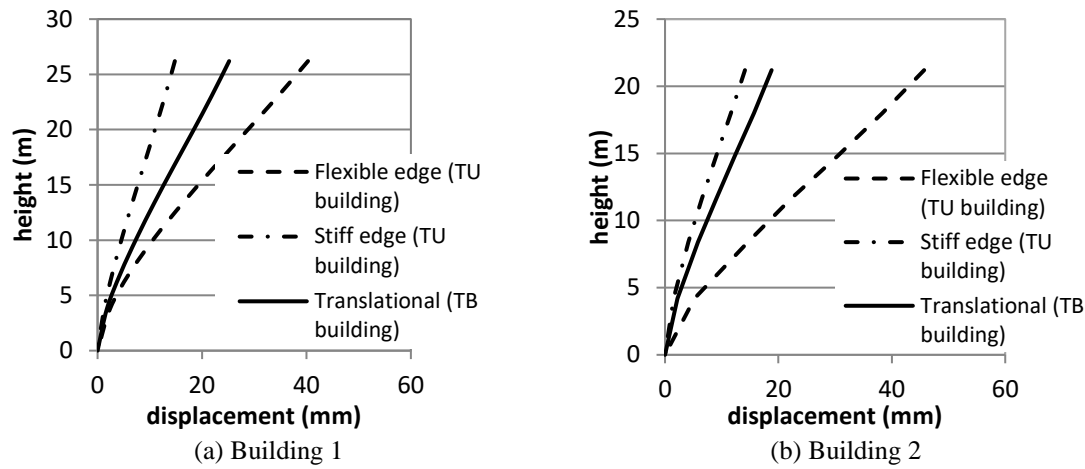


Figure 11 Displacement of TU buildings

Table 3 Eccentricity, torsional stiffness parameter and displacement ratio of the buildings

Building	$e_r$	$b_r$	$\Delta/\Delta_o$	
			Flexible edge	Stiff edge
Building 1	0.67	1.35	1.73	0.66
Building 2	0.88	0.60	2.82	0.84

The maximum displacement at the edges of the TU buildings can be estimated by multiplying the displacement ratio with the translational displacement values of the TU buildings. The translational displacement values of the buildings were obtained using the Generalised Lateral Force Method introduced by the authors (Mehdipanah *et al.*, 2016). The maximum displacement values at the edges of the TU buildings estimated using the proposed method (referred to as the Generalised Lateral Force Method herein) is plotted against the results from dynamic analyses in Figure 12. The displacement demands are also plotted in the form of inter-storey drift ratio ( $((\delta_{i+1}-\delta_i)/h_i)$ ) in Figure 13. Slightly larger discrepancies were observed for Building 2. The displacement demands of torsionally flexible buildings ( $b_r < 1.0$ ) in the acceleration and velocity-controlled range were shown to be dependent on the eccentricity and torsional stiffness parameter (Lam *et al.*, 2016). The displacement demands of Building 2 are more sensitive to variations in the values of eccentricity and torsional parameters between the floors. Nevertheless it is shown that the method provides reasonable estimates of the displacement demand of the TU buildings.

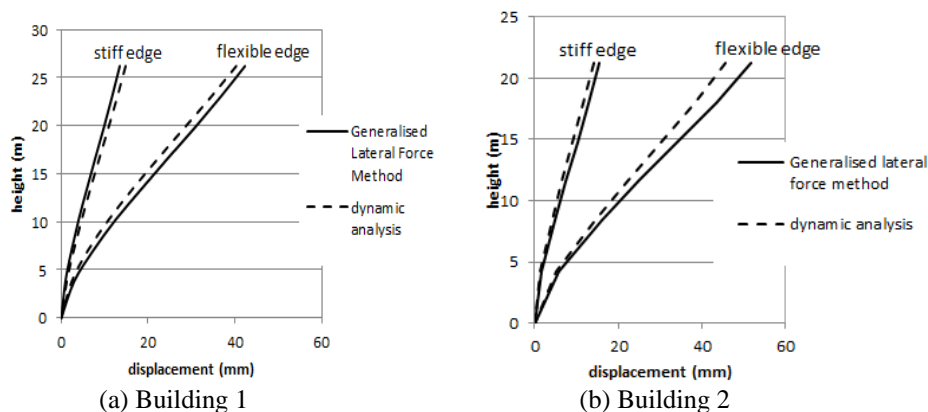


Figure 12 Displacements at the edges of TU buildings

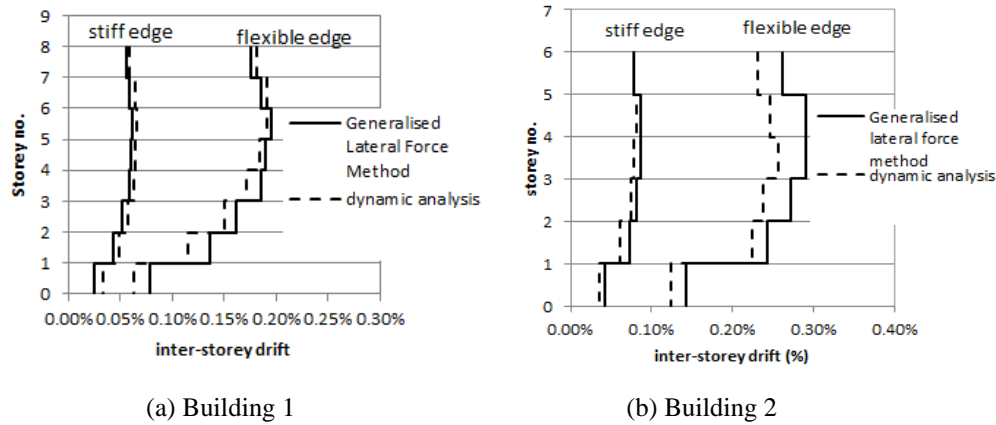


Figure 13 Inter-storey drift at the edges of TU buildings

## 5 FRAGILITY CURVES FOR THE TU BUILDINGS

Fragility curves representing the probability of the slight and moderated damage levels being exceeded were constructed. The curves were assumed to take the form of lognormal cumulative distribution function defined by Equation (8).

$$P(DS \geq ds_i | k_p Z) = \varphi \left( \frac{\ln(k_p Z) - \ln(\overline{k_p Z})}{\beta} \right) \quad (8)$$

where,  $P(DS \geq ds_i | k_p Z)$  is the probability of a ground motion with a certain level of  $k_p Z$  causing a damage level of  $ds_i$  to be exceeded,  $\overline{k_p Z}$  is the level of  $k_p Z$  that has 50% chance to cause the damage level to be exceeded and  $\beta$  is the standard deviation of the lognormal function.

The definition of damage levels and the associated inter-storey drift limits presented in Tsang et al. (2016) were adopted in the study. The parameter  $k_p Z$ , where  $k_p$  is the probability factor for the annual probability of exceedance and  $Z$  is the hazard factor, was adopted as the ground motion intensity measure. The parameter  $k_p Z$  can be easily correlated with the maximum values of response spectral velocity and was selected in view of the range of the fundamental periods of the buildings that are within the velocity controlled range of the design response spectrum. The Generalised Lateral Force Method described in Sections 2 and 3 was used to determine the  $\overline{k_p Z}$  values for the fragility curves. The method which is based on linear elastic behaviour was applied for the analysis of the buildings using the equal displacement principle (Velestos and Newmark, 1960).

The standard deviation  $\beta$  of the lognormal function is a combination of the total modelling dispersion  $\beta_M$  and the total dispersion associated with record-to-record variability  $\beta_D$ . The  $\beta_M$  value of 0.25 was adopted in the study in accordance with FEMA P-58 (ATC, 2012). The  $\beta_D$  value of 0.3 was adopted based on an earlier study conducted by the authors (Mehdipanah et al., 2016).

The fragility curves constructed for the TU buildings constructed on site class C are presented in Figures 14 and 15. The fragility curves for the equivalent TB building are also presented for comparison. It is shown in the figures that plan asymmetry in the buildings can result in significant increase in the probability of damage of the buildings. The probability of damage is also shown to be dependent on the torsional properties of the buildings. Further studies are currently being conducted to construct fragility curves for the TU buildings that represent the probability of the extensive and complete damage limit states being exceeded.

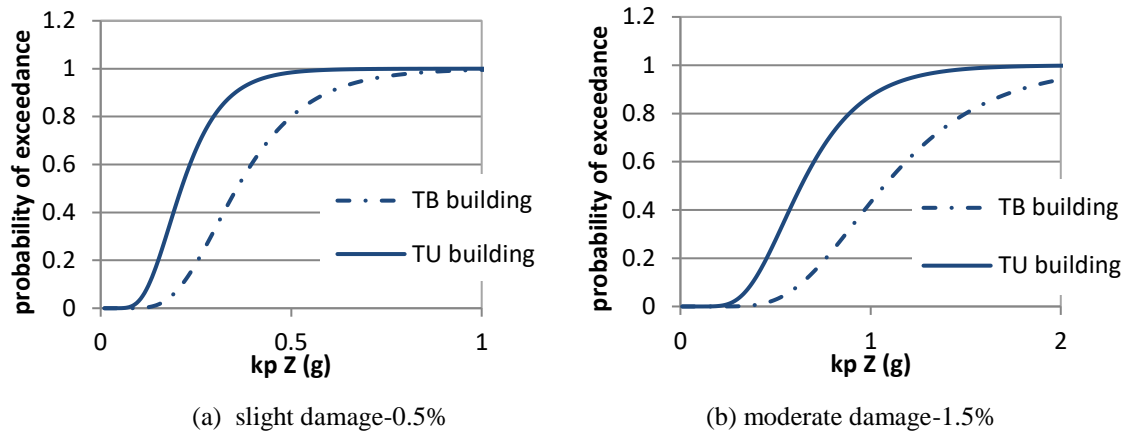


Figure 14 Fragility curves for Building 1

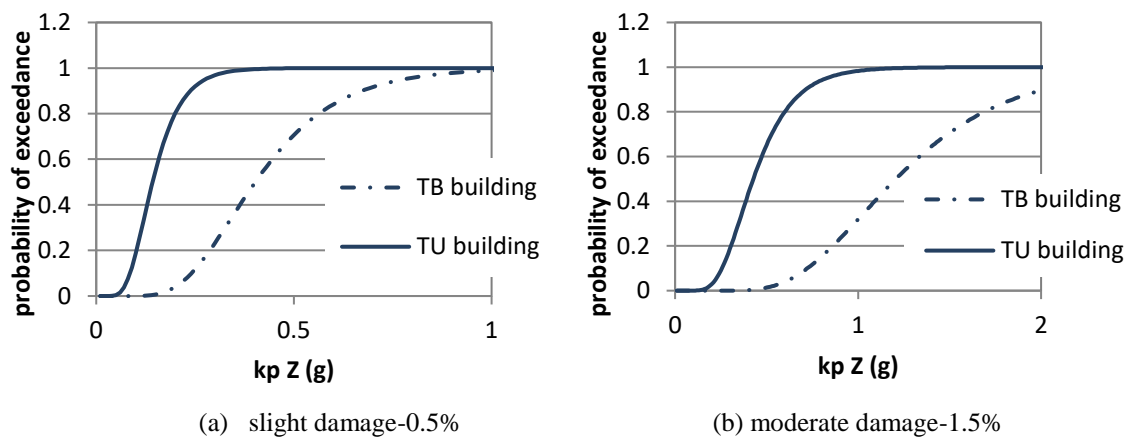


Figure 15 Fragility curves for building 2

## 6 CONCLUDING REMARKS

Many of reinforced concrete buildings in Australia feature plan asymmetry. When the center of mass does not coincide with the center of rigidity of the buildings, the displacement demand imposed on the buildings can be highly amplified, increasing their vulnerability in an earthquake.

This paper introduces a method, referred to herein as the Generalised Lateral Force Method, to provide estimates of displacement demand at the edges of multi-storey buildings featuring plan asymmetry. The method is an extension of a method previously developed by the authors for the analysis of multi-storey torsionally balanced buildings. The Generalised Lateral Force Method can provide significant time savings in the modelling and analysis of asymmetrical buildings.

The method has been verified by comparison with results from dynamic analyses of two reinforced concrete buildings featuring plan asymmetry. Fragility curves have been constructed for the two case study buildings.

## ACKNOWLEDGMENTS

The support of the Commonwealth of Australia through the Cooperative Research Centre program is acknowledged.

## REFERENCES

American Society of Civil Engineers (2000), Prestandard and commentary for the seismic rehabilitation of buildings FEMA 356, Washington, D.C.

- Anagnostopoulos, S.A., Kyrkos, M.T. and Stathopoulos, K.G. (2015) "Earthquake induced torsion in buildings: critical review and state of the art", *Earthquake and Structures*, **8**(2): 305-377.
- Applied Technology Council. 2012. Seismic performance assessment of buildings, FEMA P-58, California.
- Building Seismic Safety Council (2003), *NEHRP Recommended Provisions for Seismic Regulations for New Buildings and Other Structures Part I : Provisions (FEMA 450-1)*, Washington.
- Chandler, A.M., Duan, X.N. (1997), "Performance of asymmetric code-designed buildings for serviceability and ultimate limit states", *Earthquake Engineering and Structural Dynamics* **26**: 717-735.
- Chandler, A.M, Hutchinson, G.L. (1988), "A modified approach to earthquake resistant design of torsionally coupled buildings", *Bulletin of the New Zealand National Society of Earthquake Engineering* **21**: 140-152.
- Chopra, A.K., Goel, R.K. (1991), "Evaluation of torsional provisions in seismic code", *Journal of Structural Engineering* **117**: 3762-3782.
- Computers & Structures Inc. (2013), *User's Guide ETABS 2013: Integrated Building Design Software*, Computers & Structures, Inc, Berkeley, California, USA.
- Dempsey, K.M., Tso, W.K. (1982), "An alternative path to seismic torsional provisions", *Soil Dynamics and Earthquake Engineering* **1**: 3-10.
- EN 1998-1 (2004), *Eurocode 8: Design of structures for earthquake resistance – Part 1: General rules, seismic actions and rules for buildings*, BSI.
- Lam, N.T.K., Wilson, J.L. and Hutchinson, G.L. (1997), "Review of the torsional coupling of asymmetrical wall-frame building", *Engineering Structures* **19**(3): 233-246.
- Lam, N.T.K., Wilson, J.L. and Lumanarna, E. (2016), "Simplified elastic design checks for torsionally balanced and unbalanced low-medium rise buildings in lower seismicity regions", *Earthquakes and Structures* **11**(5): 741-777.
- Lumanarna, E., Lam, N. and Wilson, J. (2013), "Displacement-Controlled Behavior of Asymmetrical Single-Story Building Models." *Journal of Earthquake Engineering* **17**(6): 902-917.
- Mehdipanah, A., Lumanarna, E., Lam, N.T.K., Goldsworthy, H.H., Tsang, H., Wilson, J.L., Gad, E. (2016), "Seismic vulnerability assessment of irregular reinforced concrete buildings in Australia", 24th Australasian Conference on the Mechanics of Structures and Materials, Perth, Australia.
- Rutenberg, A., Pekau O.A. (1987), "Seismic code provisions for asymmetric structures: a re-evaluation", *Engineering Structures* **9**: 255-264.
- Standards Australia (2009), AS 1170.4-2007 *Structural Design Actions – Part 4 Earthquake Actions commentary*. Sydney: Standards Australia.
- Standards Australia (2007), AS 1170.4-2007 *Structural Design Actions – Part 4 Earthquake Actions commentary*. Sydney: Standards Australia.
- Tsang, H.H., Menegon, S.J., Lumanarna, E., Lam, N.T.K., Wilson, J.L., Gad, E.F., Goldsworthy, G., "Framework for seismic vulnerability assessment of reinforced concrete buildings in Australia", Australian Earthquake Engineering Society Conference 2016, Hobart, Australia.
- Tso, W.K., Zhu, T.J. (1992), "Design of torsionally unbalanced structural systems based on code provisions I: ductility demand", *Earthquake Engineering and Structural Dynamics* **21**: 609-627.
- Velestos, A.S., Newmark, N.M. (1960), "Effect of inelastic behaviour on the response of simple systems to earthquake motions", Proceedings of the Second World Conference on Earthquake Engineering, Tokyo and Kyoto, Japan.